GATA3 controls mitochondrial biogenesis in primary human CD4$^+$ T cells during DNA damage

Lauren A. Callender[1], Elizabeth C. Carroll[1], Lisa E.L. Romano[1], J. Paul Chapple[1], Arne N. Akbar[2] and Sian M. Henson[1*].

[1]Translational Medicine and Therapeutics, William Harvey Research Institute, Barts and The London School of Medicine and Dentistry, Queen Mary University of London, Charterhouse Square, London EC1M 6BQ, UK

[2]Division of Infection and Immunity, Department of Immunology, University College London, London W1T 4JF, UK

*Correspondence:

Dr. Sian M. Henson.

s.henson@qmul.ac.uk

Running title:

Keywords: T cell, GATA3, metabolism, mitochondria, senescence

Summary

GATA binding protein 3 (GATA3) has conventionally been regarded as a lineage-specific transcription factor that drives the differentiation of $CD4^+$ T helper (Th) 2 cells. However, increasing evidence shows that in addition to regulating T cell development, GATA3 is also involved in a myriad of processes such as immune regulation, proliferation and maintenance in other T cell and non-T cell lineages. Here we identify a previously unknown function for this molecule whereby in the presence of DNA damage GATA3 can induce mitochondrial biogenesis and promote mitochondrial fitness through the transcriptional coactivator peroxisome-proliferator-activated receptor γ co-activator-1α (PGC1α) in $CD4^+$ T cells. These findings extend the pleotropic nature of GATA3 and highlight the potential for GATA3-targeted cell manipulation for clinical interventions.

Introduction

The transcription factor GATA binding protein 3 (GATA3) belongs to the zinc-finger GATA (GATA-binding protein) family consisting of six members, which can be divided into further subfamilies based on their patterns of tissue expression. GATA1, -2 and -3 belong to a subfamily expressed in the haematopoietic compartment (Ko & Engel, 1993), whereas GATA4, -5 and -6 belong to a separate subfamily expressed in the developing heart, gut and smooth muscle cells (Laverriere et al., 1994; Yin & Herring, 2005).

The function of GATA3 in the development of T cells has been well characterised. It is the only member of the GATA family expressed in the T cell lineage (Ho et al., 2018). Furthermore, GATA3 deficient embryonic stem cells or haematopoietic stem cells fail to differentiate into to the T cell lineage, demonstrating that GATA3 is indispensable for T cell development (Hosoya et al., 2009; Ting, Olson, Barton, & Leiden, 1996). During early T cell development in the thymus GATA3 is essential for $CD4^+$ lineage commitment (Hernández-Hoyos, Anderson, Wang, Rothenberg, & Alberola-Ila, 2003). Moreover, mice with a conditional GATA3 knockout in mature T cells are unable to mount a T helper 2 (Th2) immune response demonstrating that among mature, peripheral $CD4^+$ T cells GATA3 is also required for Th2 differentiation (Pai, Truitt, & Ho, 2004; Zheng & Flavell, 1997; Zhu et al., 2004). Consequently, GATA3 expression has traditionally been used as a marker of Th2 cells.

More recently, GATA3 has been shown to have many functional roles beyond simply controlling $CD4^+$ Th2 cell differentiation. These roles include the development of invariant NKT (iNKT) cells (Kim et al., 2006), the maturation and homing of natural killer (NK) cells (Samson et al., 2003) and the regulation and activation of $CD8^+$ T cells (Tai, Pai, & Ho, 2012; Wang et al., 2013). Specifically, GATA3 expression has been shown to increase in $CD8^+$ T cells upon TCR activation and further increase

following cytokine stimulation (Wang et al., 2013). In addition, GATA3 deficient $CD8^+$ T cells have been shown to have defective proliferation and to have less efficient killing capabilities *in vivo* (Tai et al., 2012), highlighting the importance of GATA3 for proper $CD8^+$ T cell function. Collectively these studies expand the role of GATA3 in the $CD8^+$ T cell lineage however, the role of GATA3 in non-Th2 $CD4^+$ T cells is unknown.

We show here that GATA3 mediates mitochondrial maintenance in response to DNA damage. Highly differentiated and proliferating T cells can accumulate DNA damage as a result of increased generation of reactive oxygen species (ROS) arising as by-products of oxidative respiration (Devadas, Zaritskaya, Rhee, Oberley, & Williams, 2002; Henson et al., 2014; Kamiński et al., 2012). This is evident by the increase in yH2AX that occurs when T cells are in cell-cycle (McManus, 2005) or when they become highly differentiated (Henson et al., 2014). Cells are able to combat increased levels of ROS through ROS-quenching mechanisms (Zorov, Juhaszova, & Sollott, 2014) therefore, elevating the number of mitochondria could counteract the increase in ROS and protect the cells from further DNA damage and dysfunction. We show here a novel mechanism utilised by $CD4^+$ T cells to increase mitochondrial mass in response to DNA damage through the binding of GATA3 and PGC1α to the DNA damage repair (DDR) component ATR.

Results

GATA3 is highly expressed in CD4$^+$ EMRA T cells and positively correlates with increased mitochondrial mass

GATA3 has long been regarded as the master regulator of Th2 CD4$^+$ T cells (Zheng & Flavell, 1997). However, with differentiation CD4$^+$ T cells have been found to become more Th1 like – determined by increased IFN-γ and decreased IL-4, IL-5 and IL-13 cytokine production (Appay, Van Lier, Sallusto, & Roederer, 2008; Das et al., 2017; Sakata-Kaneko, Wakatsuki, Matsunaga, Usui, & Kita, 2000). We examined expression of GATA3 in primary human CD4$^+$ T cell subsets defined by CD45RA and CD27 expression (Supplementary figure 1) – Naive (CD45RA$^+$CD27$^+$), central memory (CM; CD45RA$^-$CD27$^+$), effector memory (EM; CD45RA$^-$CD27$^-$) and effector memory that re-express CD45RA (EMRA; CD45RA$^+$CD27$^-$) (Henson, Riddell, & Akbar, 2012; Koch et al., 2008). EMRA T cells are a highly differentiated population that exhibit many characteristics of cellular senescence such as DNA damage and increased γH2AX (Di Mitri et al., 2011). Surprisingly, CD4$^+$ EMRA T cells were found to express the highest levels of GATA3 when compared with the other three subsets despite being more Th1-like (Appay et al., 2008; Das et al., 2017; Sakata-Kaneko et al., 2000) (Figure 1a). This observation led us to hypothesize that GATA3 has an alternate function in the CD4$^+$ EMRA subset. In the CD8$^+$ lineage, GATA3 expression was low and remained unchanged amongst the four subsets (Supplementary figure 2).

Cellular metabolism is a crucial regulator of T cell function and fate. The physiological importance of mitochondria in regard to cell metabolism has been widely appreciated for many years. Therefore, we sought to investigate the mitochondrial properties of CD4$^+$ T cells subsets. Firstly, we assessed the total mitochondrial mass of CD4$^+$ T cell subsets using the mitochondrial probe; Mitotracker Green. These data revealed that mitochondrial mass increased with differentiation (Figure 1b), with CD4$^+$ EMRA T cells displaying the highest mitochondrial content (Figure 1b). This

observation was further supported by scanning electron microscopy data, which confirmed that $CD4^+$ EMRA T cells had a significantly higher volume of mitochondria (Figure 1c and d). Together with an increase in the mitochondrial mass we also observed increased expression of the co-transcriptional regulator important for mitochondrial biogenesis; PGC1α in the $CD4^+$ EMRA T cell subset (Figure 1e). Collectively these data positively correlate with the GATA3 expression data and suggested a possible link between GATA3 and mitochondrial biogenesis.

<u>$CD4^+$ EMRA T cells have hyperpolarised mitochondria but maintain normal T cell metabolism</u>

To determine whether the increased mitochondrial mass was of functional importance we used tetramethylrhodamine (TMRE) to measure mitochondrial membrane potential (ΔΨm) in $CD4^+$ T cell subsets. Notably, we observed that a greater proportion of $CD4^+$ EMRA T cells had hyperpolarised mitochondria compared with the other three subsets (Figure 2a). Hyperpolarised mitochondria have been shown to be a source of ROS in both macrophages (Mills et al., 2016) and $CD8^+$ tumour infiltrating lymphocytes (Siska et al., 2017). Therefore, we examined intracellular ROS and found that $CD4^+$ EMRA T cells also displayed high levels of ROS (Figure 2b). However, although the levels of ROS were significantly higher in the $CD4^+$ EMRA T cells compared with all other subsets, the ROS/mitochondria ratio was unchanged (Figure 2b). Therefore, the increased mitochondrial mass observed in the EMRA subset is likely a protective mechanism to ensure that $CD4^+$ EMRA T cells are able to adequately buffer the excess ROS and prevent further DNA damage (Zorov et al., 2014).

To probe this further we next investigated whether the increased mitochondrial mass and hyperpolarised mitochondrial membrane potential in $CD4^+$ EMRA T cells led to metabolic reprogramming. To do this we used a mitochondrial stress test to measure the bioenergetics profiles of TCR stimulated CD45RA/CD27 defined $CD4^+$ T cell subsets (Figure 2c). The mitochondrial stress

test includes the addition of four pharmacological drugs that manipulate oxidative phosphorylation (OXPHOS), which are added in succession to alter the bioenergetics profiles of the mitochondria.

Naïve $CD4^+$ T cells had a significantly lower basal oxygen consumption rate (OCR) compared to the memory T cells, however no differences were found amongst the three memory subsets (Figure 2d). The extracellular acidification rate (ECAR), a marker of lactic acid production and glycolysis, was highest in the EM and EMRA $CD4^+$ subsets compared to naïve and CM subsets (Figure 2e). Furthermore, the spare respiratory capacity (SRC), a measure of how well mitochondria are potentially able to produce energy under conditions of stress, was also significantly lower in the naïve $CD4^+$ T cells but unchanged in the three memory subsets (Figure 2f). Collectively, these data suggest that despite having hyperpolarised mitochondria $CD4^+$ EMRA T cells are able to maintain normal T cell metabolism.

DNA damage recruits a GATA-3-PGC1α complex to induce mitochondria biogenesis

DNA damage can severely affect the function of DNA and plays a major role in age-related diseases and cancer (Hoeijmakers, 2009). DNA damage can occur for a number of reasons. For instance, cells which undergo rapid proliferation tend to accumulate DNA damage as well as many end-stage cells that have undergone replicative senescence in response to telomere dysfunction (Harley, Futcher, & Greider, 1990; Hayflick & Moorhead, 1961; Richter & Zglinicki, 2007). In support of this we found that DNA damage, determined by an increase in the histone marker for double stranded DNA breaks; yH2AX, was significantly higher in the CD4+ EMRA T cells when compared with the other three subsets (Figure 3a). To further verify this, activation of the downstream regulator of the DNA damage response; p53 was determined by the phospho-p53/p53 ratio. Indeed, we found the amount of activated p53 increased with differentiation, with the naive $CD4^+$ T cells expressing the least and the $CD4^+$ EMRA subset expressing the most (Figure 3a).

A possible connection between GATA3 and mitochondria has been previously reported. A yeast two-hybrid screen showed that GATA3 is able to interact with the DNA damage proteins; ataxia telangiectasia mutated (ATM) and ataxia telangiectasia and Rad3-related (ATR) as well as PGC1α. Immunoprecipitation (IP) assays showed that GATA3, PGC1α and the DNA damage protein ATR existed in the same complex in $CD4^+$ EMRA T cells (Figure 3b). GATA3 was bound to the ATR in all four $CD4^+$ T cells subsets however, $CD4^+$ EMRA T cells had the highest levels of GATA3 bound to the ATR in all three repeats (Figure 3b). Little to no PGC1α was bound to the ATR in naïve and CM T cells, a small amount was bound in the EM subset however the EMRA T cell had a marked increase in the amount of PGC1α bound to the ATM/ATR (Figure 3b). These data suggest the existence of a threshold, whereby increased DNA damage together with elevated levels of GATA3 converge to recruit PGC1α and enable mitochondrial biogenesis.

To mimic DNA damage, we incubated $CD4^+$ T cells with hydroxyurea; a DNA replication inhibitor known to induce DNA double strand breaks (Bianchi, Pontis, & Reichard, 1986; Timson, 1975). Overnight incubation with hydroxyurea resulted in a significant increase in the amount of phosph-p53 (Figure 3c). Furthermore, IP assays showed that following treatment with hydroxyurea increased amounts of GATA3 and PGC1α were bound to the ATR (Figure 3d). In addition, flow cytometry analysis revealed a significant increase in intracellular PGC1α and an increased mitochondrial content, determined by elevated Mitotracker green staining (Figure 3e and f).

<u>GATA3 directly regulates $CD4^+$ T cell metabolism and mitochondrial biogenesis</u>

To verify that GATA3 can directly regulate mitochondria biogenesis and fitness we used small interfering RNA (siRNA) to reduce GATA3 expression in purified human $CD4^+$ T cells following activation (Supplementary figure 2). Transfection with GATA3 siRNA led to a significant decrease in

both the levels of PGC1α (Figure 4a) and Mitotracker Green staining (Figure 4b), signifying a marked reduction in mitochondrial mass. Confocal microscopy examination of Tom20, a major outer mitochondrial membrane receptor and therefore mitochondrial marker, showed a significant reduction in both mitochondrial mass (Figure 4d) and volume (Figure 4e) in Jurkat cells following transfection with GATA3 siRNA. TMRE staining revealed a dramatic shift from hyperpolarised to hypopolarised mitochondrial membrane potential in the GATA3 siRNA transfected $CD4^+$ T cells but not the scrambled siRNA transfected $CD4^+$ T cells (Figure 4c). Moreover, transfection with GATA3 siRNA dramatically inhibited the ability of $CD4^+$ T cells to perform OXPHOS when compared with $CD4^+$ T cells transfected with negative control scrambled siRNA (Figure 4d). Basal OCR, maximal OCR and SRC were significantly decreased in the GATA3 siRNA transfected $CD4^+$ T cells (Figure 4e, f and g). $CD8^+$ T cells transfected with GATA3 siRNA showed no difference in their bioenergetic profiles when compared with negative control scrambled siRNA (Supplementary figure 3). Taken together, these data provide evidence that GATA3 is crucial for maintaining both mitochondrial mass and fitness in $CD4^+$ T cells.

Discussion

Our data demonstrates that GATA3 plays a role in mitochondrial homeostasis in $CD4^+$ T cells. Mechanistically, we have identified that DNA damage causes elevated levels of GATA3 which interacts with PGC1α to induce mitochondrial biogenesis in $CD4^+$ T cells. Furthermore, functional analysis of $CD4^+$ T cells showed that GATA3 was crucial for T cell metabolism as GATA3 knockdown impaired mitochondrial function and abolished the cells oxidative capacity. In contrast to these findings, we have previously shown that p38 MAPK signalling in $CD8^+$ EMRA T cells resulted in a reduced mitochondrial mass, dysfunctional hypopolarised mitochondrial membranes and an impaired ability to undergo OXPHOS (Henson et al., 2014). p38 MAPK phosphorylates GATA3 enabling nuclear translocation (Maneechotesuwan et al., 2007) and while the expression of p38 is elevated in both $CD4^+$ and $CD8^+$ EMRA T cells (Di Mitri et al., 2011; Henson et al., 2014), the amount of GATA3 appears to be the dominant factor in determining the extent of mitochondrial biogenesis. Whether the increased GATA3 observed in $CD4^+$ T cells is due to a change in ubiquitination and degradation (Yamashita et al., 2005) or an enhanced level of acetylation owing to their oxidative metabolism (Cao, Rathmell, & Macintyre, 2014; Yamagata, 2000) remains to be determined.

Importantly, our observation that the GATA3-PGC1α complex is induced by DNA damage suggests that this mechanism may not be restricted to the lymphocyte lineage. Especially as GATA3 is expressed in a wide variety of tissues outside the haematopoietic system and has been implicated in the tumourigenesis of many cancers such as luminal breast cancer (Mehra et al., 2005), neuroblastoma (Peng et al., 2015), endometrial carcinomas (Engelsen, Stefansson, Akslen, & Salvesen, 2008) as well as in human T cell acute lymphoblastic leukaemia (Minegishi et al., 1997) and $CD4^+CD8^+$ double positive T cell lymphoma (van Hamburg et al., 2008).

GATA3-positive breast cancers have to been shown to be highly differentiated, with resulting tumours two-fold larger in size than control tumours (Kouros-Mehr et al., 2008). In contrast, GATA3-negative breast cancers form poorly differentiated tumours and are highly metastatic (Kouros-Mehr et al., 2008). However, despite being associated with low metastatic potential and therefore a more favourable prognosis, GATA3-positive tumours are also associated with resistance to chemotherapy (Tominaga et al., 2012). In light of the present study, we propose that the accumulation of DNA damage generated during chemotherapy recruits the GATA3-PGC1α complex, allowing GATA3-positive tumours to maintain mitochondrial fitness and evade chemotherapy induced apoptosis. However, additional examination of GATA3 and its contribution to mitochondrial biogenesis in cancer is needed to confirm this.

More broadly, our results implicate that transcription factors are likely to serve additional functions after their initial roles in differentiation. This is already the case for the Th1 differentiation marker; T-bet, which is also known to be crucial for long-term memory in $CD8^+$ T cells (Intlekofer et al., 2005; Juedes, Glimcher, Szabo, von Herrath, & Sullivan, 2003) and maturation of NK cells (Townsend et al., 2004). More recently; STAT5, which has traditionally been associated with cytokine signalling and JAK kinases (Beyer et al., 2011), has now also been identified as a central regulator of naïve $CD4^+$ T cell metabolism (Jones et al., 2019). Furthermore, although the GATA proteins have restricted expression patterns to some extent their functions can be interchangeable. For example, GATA1, - 2, and-4 can all activate the expression of GATA3 target genes IL-4 and IL-5 and repress IFNγ in T cells (Ranganath & Murphy, 2002). Interestingly, GATA4 has previously been shown to become activated in the presence of the ATM and ATR, resulting in the induction of senescence and a senescence associated secretory phenotype (SASP) in human fibroblasts (Kang et al., 2015). These functional overlaps suggest that other GATA proteins may also be capable of influencing cell metabolism.

In summary, our data identifies a previously unknown role for GATA3 in inducing mitochondrial biogenesis in response to DNA damage, revealing it as a key mediator cell metabolism. Cell types that are able to increase their levels of GATA3 in the presence of DNA damage can therefore use this mechanism as a way to protect themselves. Our findings add to the ever-expanding evidence that GATA3 is more than a marker of Th2 differentiation. Consequently, more focus should be placed on investigating the role of other transcription factors in later stages of cell development to assess their full range of their abilities.

Experimental procedures

Blood sample collection and isolation

Ethics for blood collection were approved by the NRES Committee North East (REC reference: 16/NE/0073) and all subjects provided written informed consent. Heparinized peripheral blood samples were taken from healthy volunteers, average age 41 years ± 5. Healthy volunteers were individuals who had not had an infection or immunisation within the last month, no known immunodeficiency, and had not received any other immunosuppressive medications within the last 6 months. Peripheral blood mononuclear cells (PBMCs) were isolated using Ficoll-Paque (Amersham Biosciences).

Flow cytometric analysis and cell sorting

Flow cytometric analysis was performed on approximately 1 x 106 PBMCs per sample. Cells were incubated in the dark with the Zombie_NIR live/dead stain (Biolegend) and the following antibodies: CD4 PE-CF594 (RPA-T4) from BD Biosciences, CD45RA BV605 (HI100) and CD27 BV421 (O323) from BioLegend, for 15 minutes at room temperature. For intracellular staining, the following antibodies were used: GATA3 AF488 (16E10A23) and γH2AX AF488 (2F3) from BioLegend, PGC1α (3G6), p53 Alexa Fluor 647 (1C12) and p-p53 Alexa Fluor 647 (Ser15, 16G8) from Cell Signalling Technology and goat anti-rabbit IgG H&L Alexa Fluor 488 from Abcam.

Detection of GATA3, PGC1α, p53, γH2AX and p-p53 were carried out directly ex vivo. The Foxp3 Transcription Factor Staining Buffer Kit (Biolegend) was used for staining GATA3, p53, γH2AX and p-p53. Following surface staining PBMCs were incubated with the FOXP3 Fix/Perm buffer for 20 minutes in the dark at room temperature followed by incubation with the FOXP3 Perm buffer (10X) for 15 minutes in the dark at room temperature. Finally cells were incubated with the FOXP3 Perm buffer (10X) and appropriate amount of the antibody being used for 30 minutes in the dark and

room temperature. The FIX & PERM® Cell Permeablilisation Kit (Life Technologies) was used to enable intracellular staining of PGC1α. Immediately after surface staining, PBMCs were fixed with Reagent A for 15 minutes in the dark at room temperature. Next the cells were permeabilised with Reagent B plus 10% goat serum and recommended volume of primary intracellular antibody. Cells were incubated for 20 minutes in the dark at room temperature followed by a 20 minute incubation with the secondary antibody.

All samples were acquired on a LSR Fortessa (BD Biosciences) equipped with four lasers: 488 nm blue laser, 561 nm yellow green laser, 641 red laser and 405 nm violet laser and data was analysed using FlowJo software.

$CD4^+$ T cells were purified using anti-CD4+ conjugated microbeads (Miltenyi Biotec) according to the manufacturer's instructions. Positively selected CD4+ T cells were labelled with CD27 FITC (O323) and CD45RA APC (HI100) (both from BD Biosciences) and sorted using a FACSAria (BD Biosciences). The purity of CD4 T-cell subsets were assessed by flow cytometry.

Mitochondrial measurements

For mitochondrial mass, PBMCs were incubated with 100 nM MitoTracker Green FM (Invitrogen™) for 30 minutes at 37°C, 5% CO2. ROS was measured using Dihydroethidium (DHE; ThermoFisher), 5µM MitoSOX was incubated with labelled PBMCs for 20 minutes at 37oC, 5% CO2. Mitochondrial membrane potential (MMP) was investigated using Tetramethylrhodamine (TMRE; ThermoFisher Scientific) 2 µM TMRE was incubated with PBMCs for 30 minutes at 37°C, 5% CO2. Following mitochondrial staining, samples were surface stained and then left unfixed and immediately analysed on an LSR Fortessa (BD Biosciences).

To assess mitochondrial morphology by confocal microscopy, Jurkat cells were plated onto microscope slides then fixed and permed using the FIX & PERM® Cell Permeablilisation Kit (Life Technologies) to enable intracellular labelling. Cells were incubated with Reagent A (Fixation Medium) for 15 minutes at room temperature, then Reagent B (Permeablisaton Medium) plus 10% goat serum and Tom20 (Clone??, Santa Cruz) for 20 minutes at room temperature followed incubation with the secondary antibody. Finally, cells were incubated with 4',6-diamidino-2-phenylindole (DAPI) (ThermoFisher Scientific) for 10 minutes at room temperature in the dark, and then fixed in 2% paraformaldehyde. Samples were imaged on a Zeiss LSM 880 confocal microscope with a X 63 oil-immersion objective lens. Excitation was at 488 nm from an argon-ion laser. Fluorescence detection was in the green; 500 – 570 nm and UV; 405 nm channel. Quantification of image data was performed by measuring the intensity of the 500 – 570 nm channel using ZEN-imaging. Imaris Image Analysis software was used determine mitochondrial volume through surface 3D rendering of Z-stack images.

Transmission electron microscopy studies

CD27/CD45RA defined $CD4^+$ T cell subsets were isolated and fixed in 2% paraformaldehyde, 1.5% glutaraldehyde in 0.1 m phosphate buffer pH 7.3. They were then osmicated in 1% OsO4 in 0.1M phosphate buffer, dehydrated in a graded ethanol-water series, cleared in propylene oxide and infiltrated with Araldite resin. Ultra-thin sections were cut using a diamond knife, collected on 300 mesh grids, and stained with uranyl acetate and lead citrate. The cells were viewed in a Jeol 1010 transmission electron microscope (Jeol) and imaged using a Gatan Orius CCD camera (Gatan). Mitochondrial volume density (percentage of T cell volume occupied by mitochondria) was determined from EM images using a point-counting method using image J.

Live cell metabolic assays

The Cell Mito Stress Test was performed on a Seahorse XFe96 Analyser (Agilent) to assess mitochondrial function and OXPHOS. Seahorse sensor cartridges were incubated at 37°C in a non-CO2 incubator overnight with Seahorse XF Calibrant pH 7.4 (Agilent) to rehydrate the sensor probes. The assay was performed in RPMI-1640 buffer without phenol red and carbonate buffer (Sigma-Aldrich) containing 25 mM glucose, 2 mM L-glutamine and 1 mM pyruvate with a pH of 7.4. The stress test was performed using 1 µM Oligomycin, 1.5 µM glurocarbonyl cyanide phenylydrazone (FCC), 100 nM rotenone, and 1 µM antimycin A (Agilent). Cells were stimulated with 1 µg/µL of anti-CD3 and 5 ng/mL IL-2 15 minutes prior to each metabolic test. Metabolic measurements were calculated according to the manufacturer's guidelines.

Immunoprecipitation

For immunoprecipitation experiments the Chk1 antibody was incubated with Red Protein G Affinity beads (Sigma-Aldrich) for 1 hour at 4°C on a shaker to allow the antibody to bind to the beads. Cell lysates were collectted in RIPA buffer plus inhibitors (protease: complete mini Roche; 11836153001, and phosphatases: cocktail set II Calbiochem; 524625) and then incubated with the antibody-bead mix overnight at 4°C on a shaker. The following morning, samples were centrifuged, and the supernatant was discarded leaving only the proteins able to bind to Chk1. SDS-polyacrylamide electrophoresis and western blotting of GATA3 and PGC1α was then carried performed as described above. The protein was detected via chemiluminescence, by means of the ECL system (GE Healthcare).

Hydroxyurea experiments

To induce DNA damage, PBMCs were incubated with 400 µM hydroxyurea for 48 hours. Following DNA damage cells an immunoprecipitation using the Chk1 antibody was carried out to assess GATA3 and PGC1 binding and mitochondrial properties were examined via flow cytometry.

GATA3 siRNA knockdown experiments

GATA-3 and scrambled siRNA (GATA3; 5'-/5Alex647N/UAG GCG AAU CAU UUG UUC AAA-3', Scrambled; 5' CCU GUU CUU AAA AUA GUA GGC 3') were dissolved to a final concentration of 10 µM in electroporation buffer, transferred to an electroporation cuvette and electroporated using program T-023 on an Amaxa Nucleofector (Lonza Bioscience). Cell were then left to recover for 24 to 48 hours in fresh RPMI-1640 media. Primary human CD4+ T cells were stimulated with 1 µg/µL of anti-CD3 and 5 ng/mL IL-2 for 24 hours prior to transfection whereas Jurkat cells were left unstimulated.

Statistical analysis

GraphPad Prism was used to perform statistical analysis. Statistical significance was evaluated using the paired Student t-test or a repeated-measures ANOVA with the Tukey correction used for post hoc testing. Differences were considered significant when P was <0.05.

Acknowledgements

This work was supported by the British Heart Foundation (LAC), a Springboard award from the Academy of Medical Science and the Wellcome trust (ECC, SMH), the Rosetrees Trust (SMH). ANA was funded by the Medical Research Council (MR/P00184X/1). We would also like to thank the CRUK Flow Cytometry Core Service at Barts Cancer Institute (Core Award C16420/A18066). The LSM880 confocal used in these studies was purchased through a Barts and the London Charity grant MGU0293.

Conflict of Interest

The authors have no conflicting financial interests.

Author contributions

LAC and SMH wrote the manuscript, performed the experiments and analysed the data; ECC performed experiments; LELR and JPC assisted with the Tom20 experiments and reviewed the manuscript and ANA reviewed the manuscript.

References

Appay, V., Van Lier, R. A. W., Sallusto, F., & Roederer, M. (2008). Phenotype and function of human T lymphocyte subsets: Consensus and issues. *Cytometry Part A*.

Beyer, T., Busse, M., Hristov, K., Gurbiel, S., Smida, M., Haus, U. U., … Lindquist, J. A. (2011). Integrating signals from the T-cell receptor and the interleukin-2 receptor. *PLoS Comp Biol.*

Bianchi, V., Pontis, E., & Reichard, P. (1986). Changes of deoxyribonucleoside triphosphate pools induced by hydroxyurea and their relation to DNA synthesis. *J Biol Chem*.

Cao, Y., Rathmell, J. C., & Macintyre, A. N. (2014). Metabolic reprogramming towards aerobic glycolysis correlates with greater proliferative ability and resistance to metabolic inhibition in CD8 versus CD4 T cells. *PLoS ONE*.

Das, A., Ranganathan, V., Umar, D., Thukral, S., George, A., Rath, S., & Bal, V. (2017). Effector/memory CD4 T cells making either Th1 or Th2 cytokines commonly co-express T-bet and GATA-3. *PLoS ONE*.

Devadas, S., Zaritskaya, L., Rhee, S. G., Oberley, L., & Williams, M. S. (2002). Discrete Generation of Superoxide and Hydrogen Peroxide by T Cell Receptor Stimulation: Selective Regulation of Mitogen-Activated Protein Kinase Activation and Fas Ligand Expression. *J. Exp. Med*.

Di Mitri, D., Azevedo, R. I., Henson, S. M., Libri, V., Riddell, N. E., Macaulay, R., Kipling, D., Soares, M. V., Battistini, L., Akbar, A. N. (2011). Reversible Senescence in Human CD4+CD45RA+CD27- Memory T Cells. *J Immunol*.

Engelsen, I. B., Stefansson, I. M., Akslen, L. A., & Salvesen, H. B. (2008). GATA3 expression in estrogen receptor α-negative endometrial carcinomas identifies aggressive tumors with high proliferation and poor patient survival. *Am J Obstet Gynecol*.

Harley, C. B., Futcher, A. B., & Greider, C. W. (1990). Telomeres shorten during ageing of human fibroblasts. *Nature*.

Hayflick, L., & Moorhead, P. S. (1961). The serial cultivation of human diploid cell strains. *Expl Cell*

Res.

Henson, S. M., Lanna, A., Riddel, N. E., Franzese, O., Macaulay, R., Griffiths, S. J., Puleston, D. J., Watson, A. S., Simon, A. K., Tooze, S. A., Akbar, A. N. (2014). P38 signaling inhibits mTORC1-independent autophagy in senescent human CD8+ T cells. *J Clin Invest*.

Henson, S. M., Riddell, N. E., & Akbar, A. N. (2012). Properties of end-stage human T cells defined by CD45RA re-expression. *Curr Opin Immunol*.

Hernández-Hoyos, G., Anderson, M. K., Wang, C., Rothenberg, E. V., & Alberola-Ila, J. (2003). GATA-3 expression is controlled by TCR signals and regulates CD4/CD8 differentiation. *Immunity*.

Ho, I. C., Vorhees, P., Marin, N., Oakley, B. K., Orkin, S. H., Leiden, J. M., & Tsai, S. F. (2018). Human GATA-3: a lineage-restricted transcription factor that regulates the expression of the T cell receptor alpha gene. *EMBO J*.

Hoeijmakers, J. H. J. (2009). DNA Damage, Aging, and Cancer. *New Eng J Med*.

Hosoya, T., Kuroha, T., Maillard, I., Moriguchi, T., Engel, J. D., Cummings, D., & Lim, K.-C. (2009). GATA-3 is required for early T lineage progenitor development. *J Exp Med*.

Intlekofer, A. M., Takemoto, N., Wherry, E. J., Longworth, S. A., Northrup, J. T., Palanivel, V. R., … Reiner, S. L. (2005). Effector and memory CD8+ T cell fate coupled by T-bet and eomesodermin. *Nat Immunol*.

Jones, N., Vincent, E. E., Cronin, J. G., Panetti, S., Chambers, M., Holm, S. R., Owens, S. E., Francis, N. J., Finlay, D. K., Thornton, C. A. (2019). Akt and STAT5 mediate naïve human CD4+ T-cell early metabolic response to TCR stimulation. *Nat Comms*.

Juedes, A., Glimcher, L. H., Szabo, S. J., von Herrath, M., & Sullivan, B. M. (2003). Antigen-driven effector CD8 T cell function regulated by T-bet. *Proc Nat Acad Sci*.

Kamiński, M. M., Sauer, S. W., Kamiński, M., Opp, S., Ruppert, T., Grigaravičius, P., … Gülow, K. (2012). T cell Activation Is Driven by an ADP-Dependent Glucokinase Linking Enhanced

Glycolysis with Mitochondrial Reactive Oxygen Species Generation. *Cell Rep*.

Kang, C., Xu, Q., Martin, T. D., Li, M. Z., Demaria, M., Aron, L., … Elledge, S. J. (2015). The DNA damage response induces inflammation and senescence by inhibiting autophagy of GATA4. *Science*.

Kim, P. J., Pai, S. Y., Brigl, M., Besra, G. S., Gumperz, J., & Ho, I. C. (2006). GATA-3 regulates the development and function of invariant NKT cells. *J Immunol*.

Ko, L. J., & Engel, J. D. (1993). DNA-binding specificities of the GATA transcription factor family. *Mol Cell Biol*.

Koch, S., Larbi, A., Derhovanessian, E., Özcelik, D., Naumova, E., & Pawelec, G. (2008). Multiparameter flow cytometric analysis of CD4 and CD8 T cell subsets in young and old people. *Immunity and Ageing*.

Kouros-Mehr, H., Bechis, S. K., Slorach, E. M., Littlepage, L. E., Egeblad, M., Ewald, A. J., … Werb, Z. (2008). GATA-3 Links Tumor Differentiation and Dissemination in a Luminal Breast Cancer Model. *Cancer Cell*.

Laverriere, A. C., MacNeill, C., Mueller, C., Poelmann, R. E., Burch, J. B. E., & Evans, T. (1994). GATA-4/5/6, a subfamily of three transcription factors transcribed in developing heart and gut. *J Biol Chem*.

Maneechotesuwan, K., Xin, Y., Ito, K., Jazrawi, E., Lee, K.-Y., Usmani, O. S., … Adcock, I. M. (2007). Regulation of Th2 Cytokine Genes by p38 MAPK-Mediated Phosphorylation of GATA-3. *J Immunol*.

McManus, K. J. (2005). ATM-dependent DNA Damage-independent Mitotic Phosphorylation of H2AX in Normally Growing Mammalian Cells. *Mol Biol Cell*.

Mehra, R., Varambally, S., Ding, L., Shen, R., Sabel, M. S., Ghosh, D., … Kleer, C. G. (2005). Identification of GATA3 as a breast cancer prognostic marker by global gene expression meta-analysis. *Cancer Res*.

Mills, E. L., Kelly, B., Logan, A., Costa, A. S. H., Varma, M., & Bryant, C. E. (2016). Repurposing mitochondria from ATP production to ROS generation drives a pro-inflammatory phenotype in macrophages that depends on succinate oxidation by complex II. *Cell*.

Minegishi, N., Morita, S., Minegishi, M., Tsuchiya, S., Konno, T., Hayashi, N., & Yamamoto, M. (1997). Expression of GATA transcription factors in myelogenous and lymphoblastic leukemia cells. *Int J Hematol. 65*(3), 239–249.

Pai, S.-Y., Truitt, M. L., & Ho, I.-C. (2004). GATA-3 deficiency abrogates the development and maintenance of T helper type 2 cells. *Proc Nat Acad Sci*.

Peng, H., Ke, X. X., Hu, R., Yang, L., Cui, H., & Wei, Y. (2015). Essential role of GATA3 in regulation of differentiation and cell proliferation in SK-N-SH neuroblastoma cells. *Mol Med Rep*.

Ranganath, S., & Murphy, K. M. (2002). Structure and Specificity of GATA Proteins in Th2 Development. *Mol Cell Biol*.

Richter, T., & Zglinicki, T. von. (2007). A continuous correlation between oxidative stress and telomere shortening in fibroblasts. *Exp Gerontol*.

Sakata-Kaneko, S., Wakatsuki, Y., Matsunaga, Y., Usui, T., & Kita, T. (2000). Altered Th1/Th2 commitment in human CD4+ T cells with ageing. *Clin Exp Immunol*.

Samson, S. I., Richard, O., Tavian, M., Ranson, T., Vosshenrich, C. A. J., Colucci, F., … Di Santo, J. P. (2003). GATA-3 promotes maturation, IFN-γ production, and liver-specific homing of NK cells. *Immunity*.

Siska, P. J., Beckermann, K. E., Mason, F. M., Andrejeva, G., Greenplate, A. R., Sendor, A. B., … Rathmell, J. C. (2017). Mitochondrial dysregulation and glycolytic insufficiency functionally impair CD8 T cells infiltrating human renal cell carcinoma. *JCI Insight*.

Tai, T.-S., Pai, S.-Y., & Ho, I.-C. (2012). GATA-3 Regulates the Homeostasis and Activation of CD8+ T Cells. *J Immunol*.

Timson, J. (1975). Hydroxyurea. *Mutation Res. 32*(2), 115–132.

Ting, C. N., Olson, M. C., Barton, K. P., & Leiden, J. M. (1996). Transcription factor GATA-3 is required for development of the T-cell lineage. *Nature*.

Tominaga, N., Naoi, Y., Shimazu, K., Nakayama, T., Maruyama, N., Shimomura, A., … Noguchi, S. (2012). Clinicopathological analysis of GATA3-positive breast cancers with special reference to response to neoadjuvant chemotherapy. *Ann Oncol*.

Townsend, M. J., Weinmann, A. S., Matsuda, J. L., Salomon, R., Farnham, P. J., Biron, C. A., … Glimcher, L. H. (2004). T-bet regulates the terminal maturation and homeostasis of NK and Vα14i NKT cells. *Immunity*.

van Hamburg, J. P., de Bruijn, M. J. W., Dingjan, G. M., Beverloo, H. B., Diepstraten, H., Ling, K. W., & Hendriks, R. W. (2008). Cooperation of Gata3, c-Myc and Notch in malignant transformation of double positive thymocytes. *Mol Immunol*.

Wang, Y., Misumi, I., Gu, A. Di, Curtis, T. A., Su, L., Whitmire, J. K., & Wan, Y. Y. (2013). GATA-3 controls the maintenance and proliferation of T cells downstream of TCR and cytokine signaling. *Nat Immunol*.

Yamagata, T. (2000). Acetylation of GATA-3 affects T-cell survival and homing to secondary lymphoid organs. *EMBO J*.

Yamashita, M., Shinnakasu, R., Asou, H., Kimura, M., Hasegawa, A., Hashimoto, K., … Nakayama, T. (2005). Ras-ERK MAPK cascade regulates GATA3 stability and Th2 differentiation through ubiquitin-proteasome pathway. *J Biol Chem*.

Yin, F., & Herring, B. P. (2005). GATA-6 can act as a positive or negative regulator of smooth muscle-specific gene expression. *J Biol Chem*.

Zheng, W. P., & Flavell, R. A. (1997). The transcription factor GATA-3 is necessary and sufficient for Th2 cytokine gene expression in CD4 T cells. *Cell*.

Zhu, J., Min, B., Hu-Li, J., Watson, C. J., Grinberg, A., Wang, Q., … Paul, W. E. (2004). Conditional deletion of Gata3 shows its essential function in TH1-TH2 responses. *Nat Immunol*.

Zorov, D. B., Juhaszova, M., & Sollott, S. J. (2014). Mitochondrial Reactive Oxygen Species (ROS) and ROS-Induced ROS Release. *Physiol Rev*.

Figure legends

Figure 1: Senescent CD4$^+$ EMRA T cells expressed high levels of GAT3 which correlates with increased mitochondrial mass.

(a) Representative flow cytometry histograms and cumulative graph of GATA3 staining in CD27/CD45RA defined CD4$^+$ T cell subsets (*n* = 7). (b) Representative flow cytometry histograms and cumulative graph of Mitotraker Green staining in CD27/CD45RA defined CD4$^+$ T cell subsets (*n* = 14). (c) Electron microscope images of CD27/CD45RA defined CD4$^+$ T cell subsets imaged directly *ex vivo*. Scale bars 1 µM. (d) Graph shows the percentage by cell volume of mitochondria in CD27/CD45RA defined CD4$^+$ T cell subsets determined by a point counting grid method from 20 different electron microscope images. (e) PGC1α staining in CD45RA/CD27 defined CD4$^+$ T cell subsets (*n* = 8).

Figure 2: CD4$^+$ EMRA T cells have hyperpolarised mitochondria but maintain normal T cell metabolism.

(a) Mitochondrial membrane potential (MMP) was determined in CD27/CD45RA defined CD4+ T cell subsets using TMRE (*n* = 10). Low MMP = red, intermediate MMP = blue, high MMP = green. (b) ROS production was obtained using DHE in the CD27/CD45RA defined CD4$^+$ T cell subsets (*n* = 7). (c) OCR of the CD4$^+$ T cell subsets was measured after 15 minute stimulation with 0.5 µg/ml anti-CD3 and 5 ng/ml IL-2, cells were subjected to a mitochondrial stress test using indicated mitochondrial inhibitors. Data are representative of 4 independent experiments. (d) Basal OCR, (e) Basal ECAR and (f) the SRC of the CD4$^+$ T cell subsets after 15 minute stimulation with 0.5 µg/ml anti-CD3 and 5 ng/ml IL-2 (*n* = 4).

Figure 3: DNA damage recruits a GATA-3-PGC1α complex to induce mitochondria biogenesis in CD4$^+$ EMRA T cells.

(a) DNA damage in the CD27/CD45RA defined $CD4^+$ T cell subsets was determined by assessing the percentage of yH2AX positive cells and the p53:p-p53 ratio. (b) Representative image of western blot after Chk1 immunoprecipitation in the CD27/CD45RA defined $CD4^+$ T cell subsets and cumulative graphs to quantify the amount of GATA3 and PGC1α bound to the Chk1 antibody (*n* = 3). (e) The p53:p-p53 ratio following the induction of DNA damage by hydroxyurea in whole $CD4^+$ T cells. (d) Representative image of western blot after Chk1 immunoprecipitation in $CD4^+$ T cells treated with and without hydroxyurea and cumulative graphs to quantify the amount of GATA3 and PGC1α bound to the Chk1 antibody (*n* = 3). (e) PGC1α and (f) Mitotracker Green staining in $CD4^+$ T cells treated with and without hydroxyurea.

Figure 4: GATA3 directly regulates $CD4^+$ T cell metabolism and mitochondrial biogenesis.

Representative flow cytometry histograms and cumulative graph of (a) PGC1α and (b) Mitotracker Green staining in whole $CD4^+$ T cells transfected with either –ve control or GATA3 siRNA (*n* = 5 and 6 respectively). (c) Tom20 staining in Jurkat T cells transfected with either –ve control or GATA3 siRNA was determined (d) mitochondrial mass (e) and mitochondrial volume by confocal microscopy (Data from 3 independent experiments). (f) MMP was determined in whole $CD4^+$ T cells transfected with either –ve control or GATA3 siRNA using TMRE (*n* = 6). Low MMP = red, intermediate MMP = blue, high MMP = green. (g) OCR of whole CD4+ T cells transfected with either –ve control or GATA3 siRNA was measured after 15 minute stimulation with 0.5 µg/ml anti-CD3 and 5 ng/ml IL-2, cells were subjected to a mitochondrial stress test using indicated mitochondrial inhibitors. Data are representative of 3 independent experiments. (h) Basal OCR and (i) the SRC of the $CD4^+$ siRNA transfected cells after 15 minute stimulation with 0.5 µg/ml anti-CD3 and 5 ng/ml IL-2 (*n* = 3).

Figure 1.

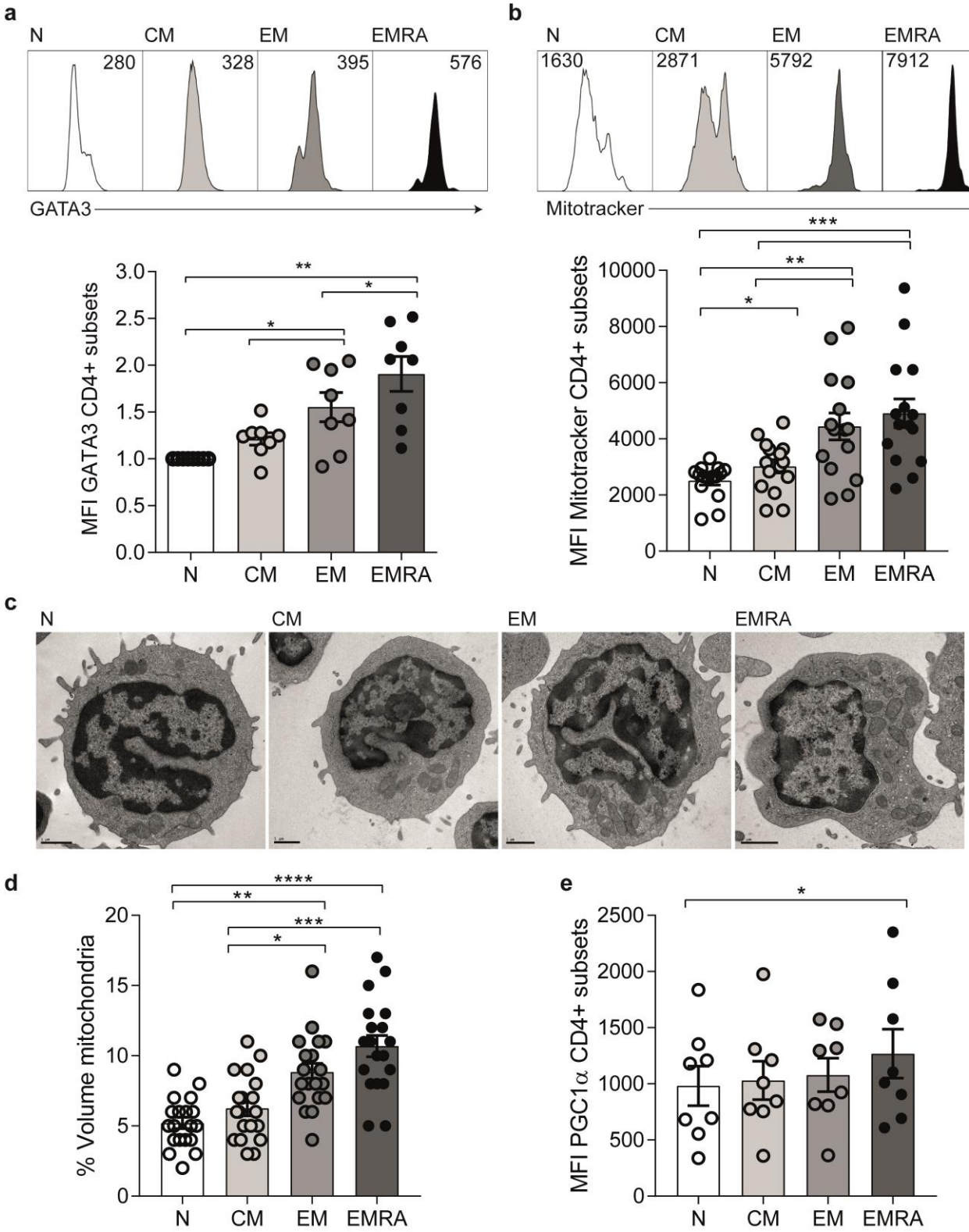
a
N
CM
EM
EMRA
280
328
395
576
GATA3
MFI GATA3 CD4+ subsets
3.0
2.5
2.0
1.5
1.0
0.5
0.0
**
*
*
N
CM
EM
EMRA
b
N
CM
EM
EMRA
1630
2871
5792
7912
Mitotracker
MFI Mitotracker CD4+ subsets
10000
8000
6000
4000
2000
0
***
**
*
N
CM
EM
EMRA
c
N
CM
EM
EMRA
d
% Volume mitochondria
20
15
10
5
0
****
**
***
*
N
CM
EM
EMRA
e
MFI PGC1α CD4+ subsets
2500
2000
1500
1000
500
0
*
N
CM
EM
EMRA

Figure 2.

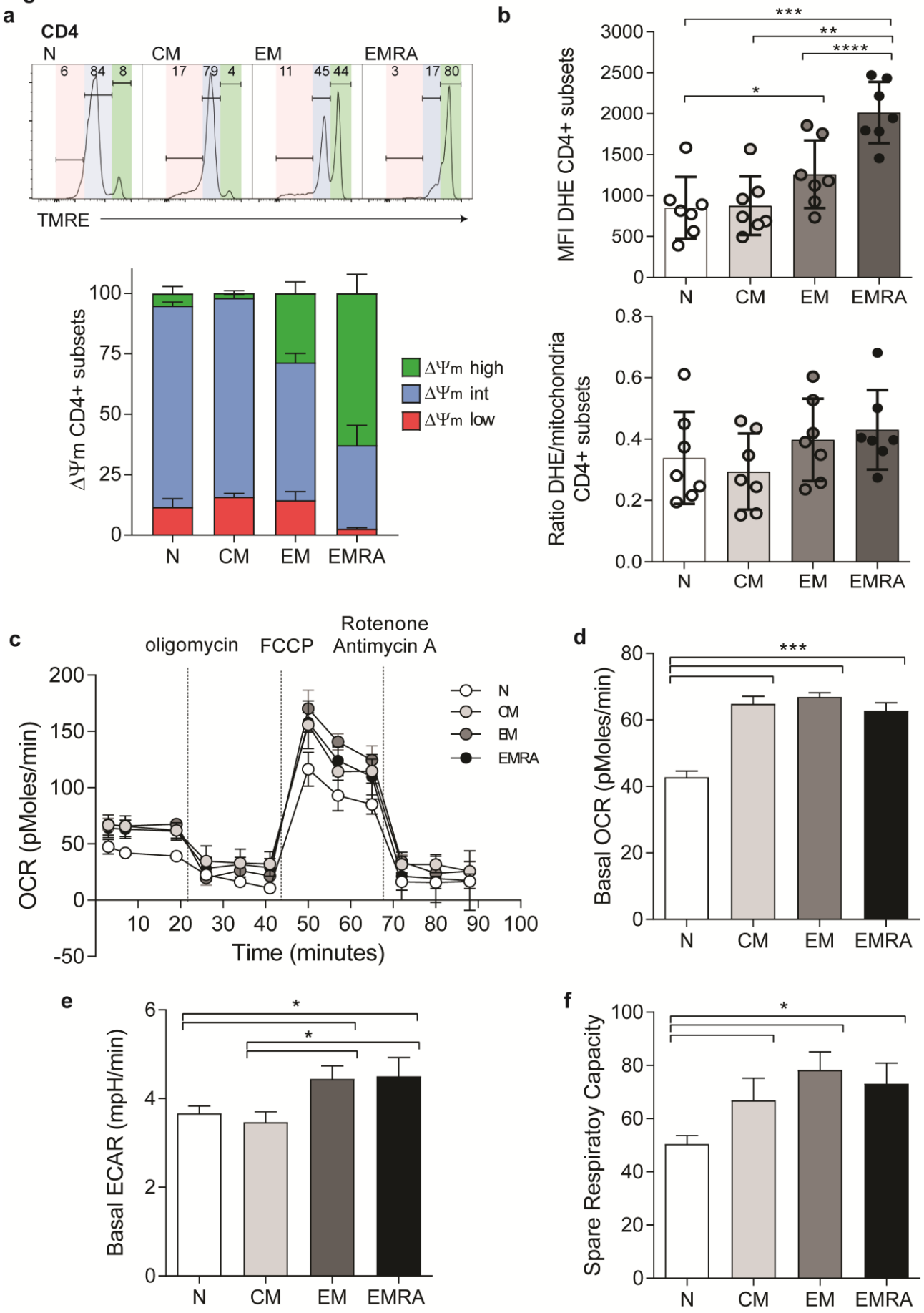
a
CD4
N
CM
EM
EMRA
6
84
8
17
79
4
11
45
44
3
17
80
TMRE
ΔΨm CD4+ subsets
ΔΨm high
ΔΨm int
ΔΨm low
b
MFI DHE CD4+ subsets
Ratio DHE/mitochondria CD4+ subsets
c
oligomycin
FCCP
Rotenone
Antimycin A
OCR (pMoles/min)
Time (minutes)
d
Basal OCR (pMoles/min)
e
Basal ECAR (mpH/min)
f
Spare Respiratoy Capacity

Figure 3.

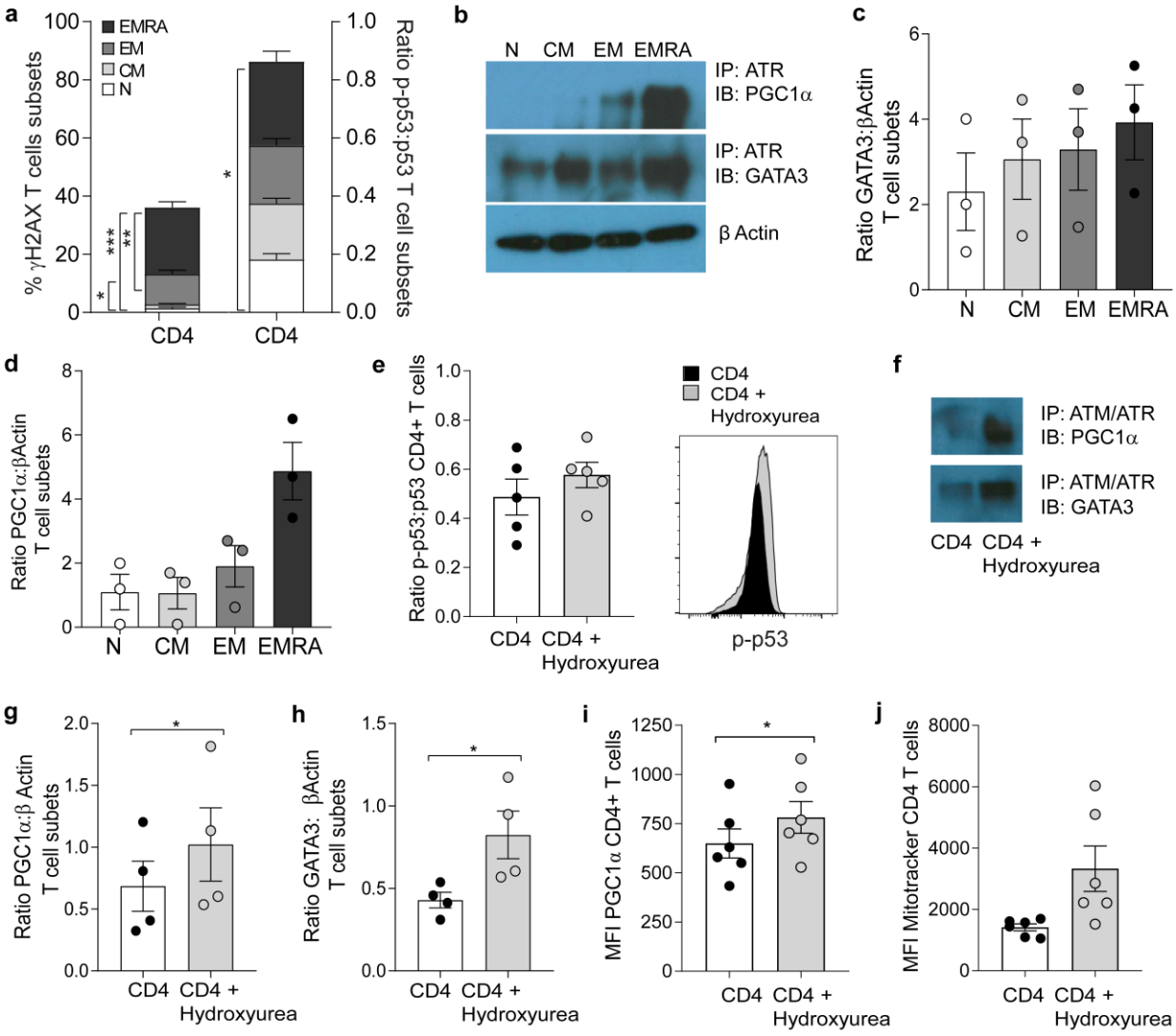
a
EMRA
EM
CM
N
% γH2AX T cells subsets
Ratio p-p53:p53 T cell subsets
CD4
CD4
b
N CM EM EMRA
IP: ATR
IB: PGC1α
IP: ATR
IB: GATA3
β Actin
c
Ratio GATA3:βActin T cell subets
N CM EM EMRA
d
Ratio PGC1α:βActin T cell subets
N CM EM EMRA
e
Ratio p-p53:p53 CD4+ T cells
CD4
CD4 + Hydroxyurea
p-p53
f
IP: ATM/ATR
IB: PGC1α
IP: ATM/ATR
IB: GATA3
CD4 CD4 + Hydroxyurea
g
Ratio PGC1α:β Actin T cell subets
h
Ratio GATA3: βActin T cell subets
i
MFI PGC1α CD4+ T cells
j
MFI Mitotracker CD4 T cells
CD4 CD4 + Hydroxyurea

Figure 4.

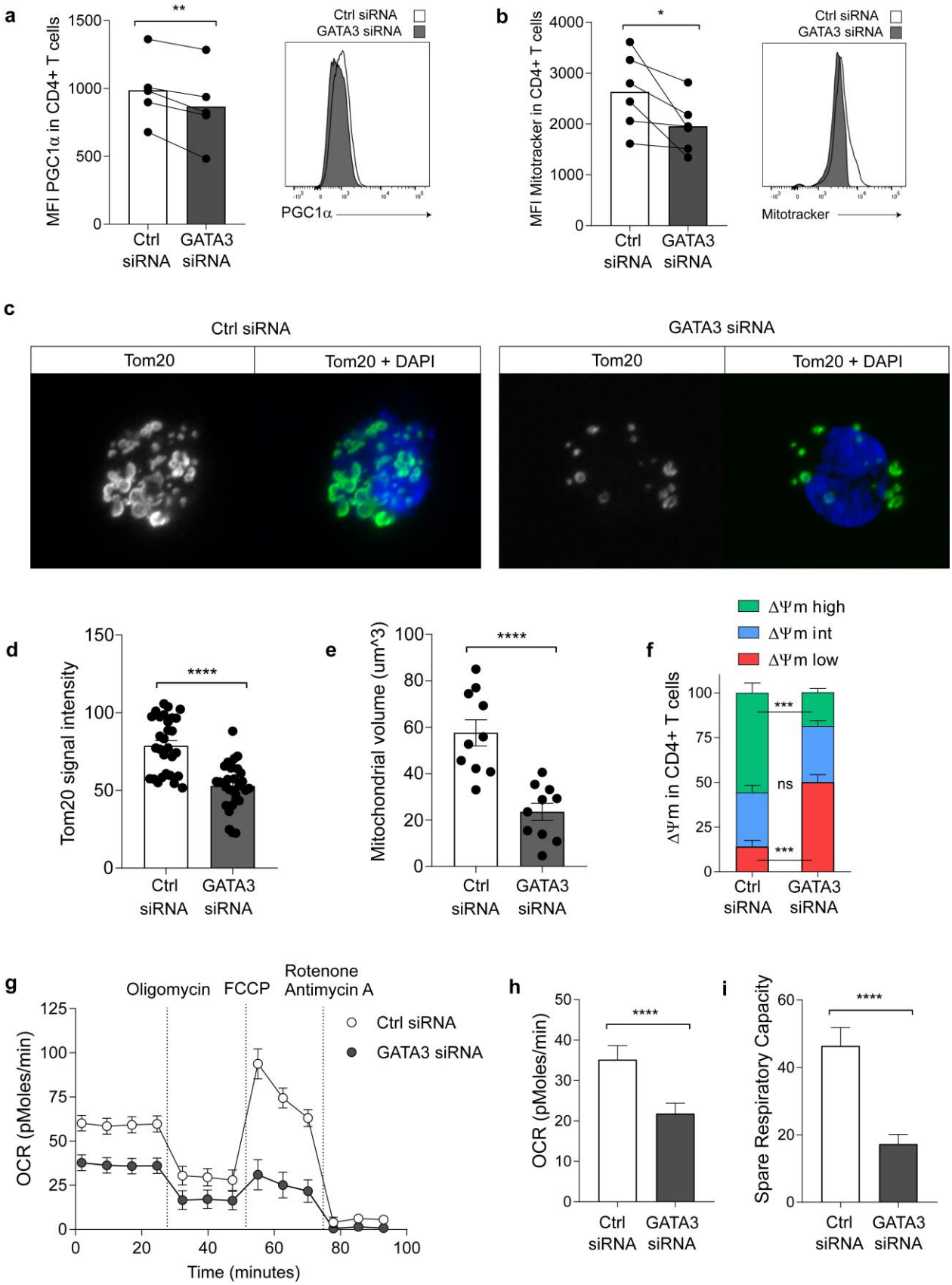
a
MFI PGC1α in CD4+ T cells
1500
1000
500
0
**
Ctrl siRNA
GATA3 siRNA
Ctrl siRNA
GATA3 siRNA
PGC1α
b
MFI Mitotracker in CD4+ T cells
4000
3000
2000
1000
0
*
Ctrl siRNA
GATA3 siRNA
Ctrl siRNA
GATA3 siRNA
Mitotracker
c
Ctrl siRNA
Tom20
Tom20 + DAPI
GATA3 siRNA
Tom20
Tom20 + DAPI
d
Tom20 signal intensity
150
100
50
0
****
Ctrl siRNA
GATA3 siRNA
e
Mitochondrial volume (um^3)
100
80
60
40
20
0
****
Ctrl siRNA
GATA3 siRNA
f
ΔΨm high
ΔΨm int
ΔΨm low
ΔΨm in CD4+ T cells
100
75
50
25
0
***
ns
***
Ctrl siRNA
GATA3 siRNA
g
Oligomycin
FCCP
Rotenone
Antimycin A
Ctrl siRNA
GATA3 siRNA
OCR (pMoles/min)
125
100
75
50
25
0
0
20
40
60
80
100
Time (minutes)
h
OCR (pMoles/min)
50
40
30
20
10
0
****
Ctrl siRNA
GATA3 siRNA
i
Spare Respiratory Capacity
60
40
20
0
****
Ctrl siRNA
GATA3 siRNA

Supplementary figure legends

Supplementary figure 1: Gating strategy for CD27/CD45RA defined $CD4^+$ T cell subsets.

(a) Lymphocytes, (b) single cells, (C) live cells, (D) CD4+ T cells and (E) CD27/CD45RA subsets.

Supplementary figure 2: GATA3 expression in CD27/CD45RA defined $CD8^+$ T cell subsets.

Supplementary figure 3: siRNA knockdown efficiency

(a) GATA3 siRNA transfection efficiency (n = 6). (b) GATA3 staining following GATA3 siRNA transfection (n = 3). (c) Percentage of live cells determined by Zombie NIR staining following GATA3 siRNA transfection (n = 6).

Supplementary figure 4: OCR of whole $CD8^+$ T cells transfected with either –ve control or GATA3 siRNA was measured after 15 minute stimulation with 0.5 µg/ml anti-CD3 and 5 ng/ml IL-2, cells were subjected to a mitochondrial stress test using indicated mitochondrial inhibitors. Data are representative of 3 independent experiments.

Supplementary figure 1.

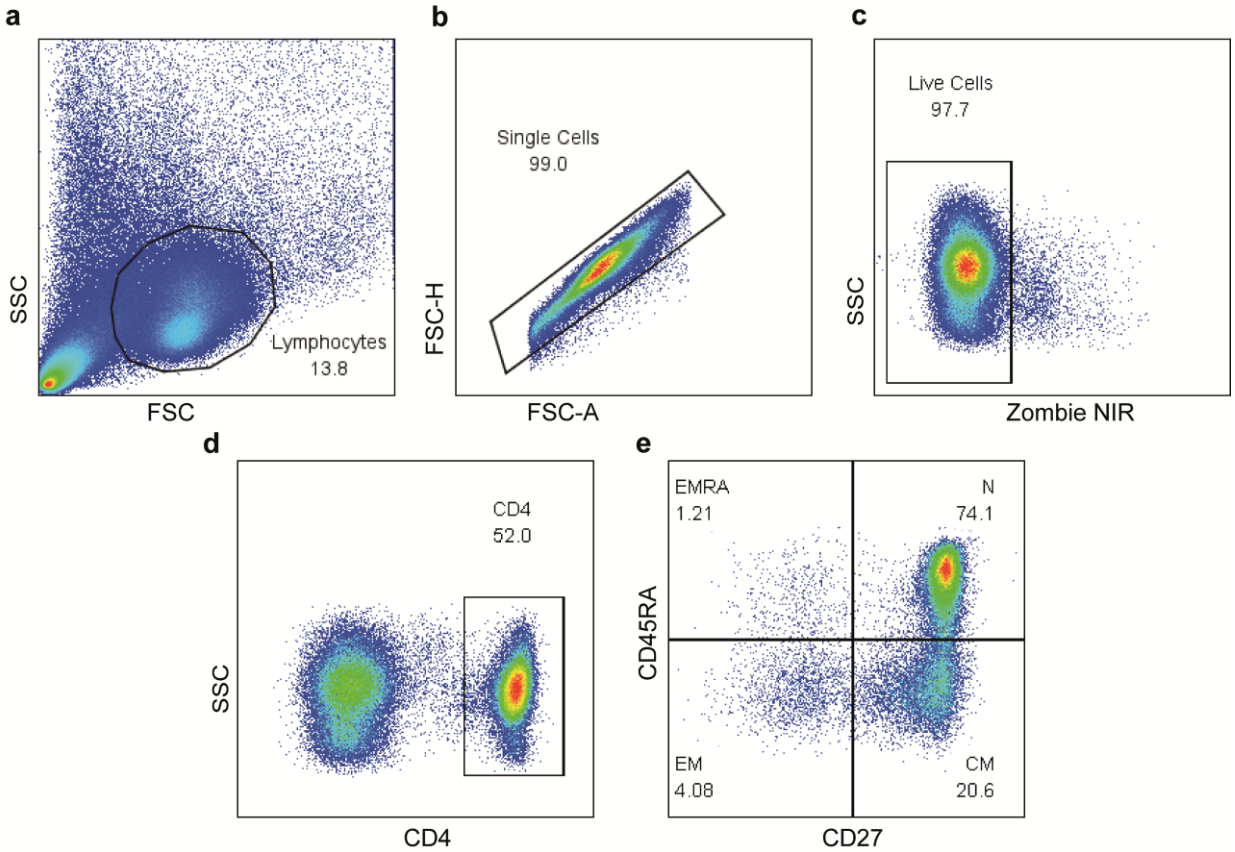

Supplementary figure 2.

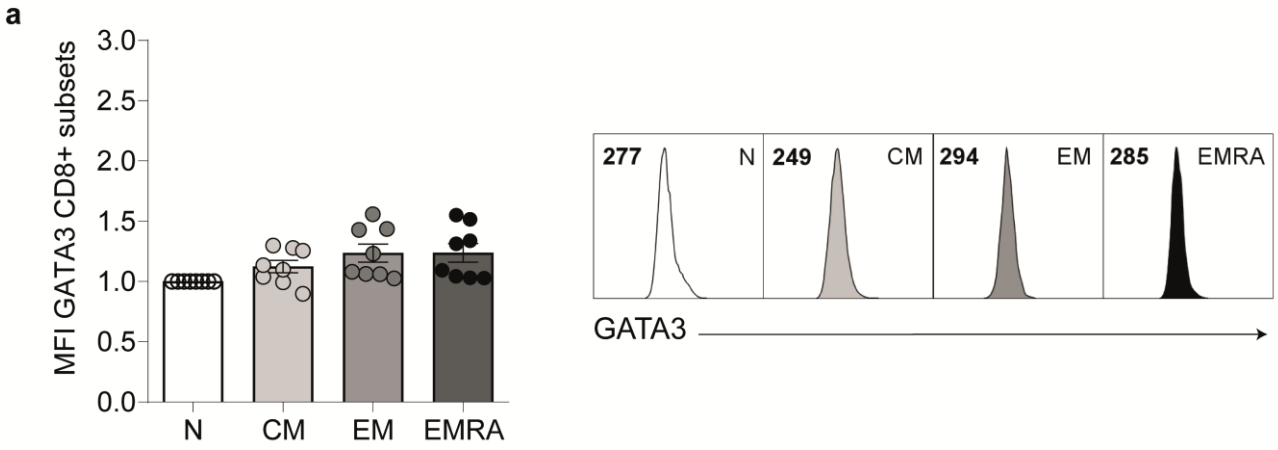

Supplementary figure 3.

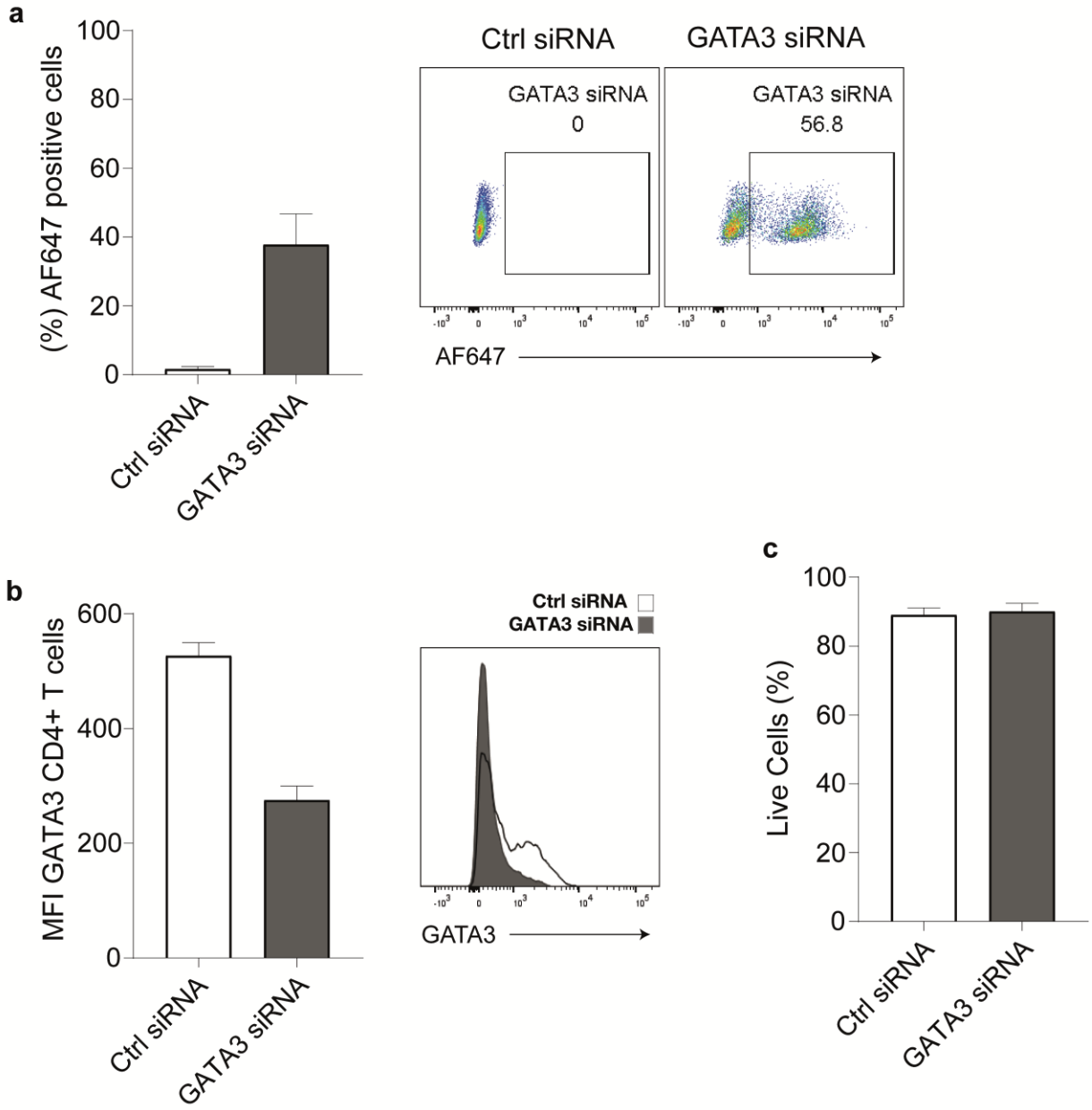
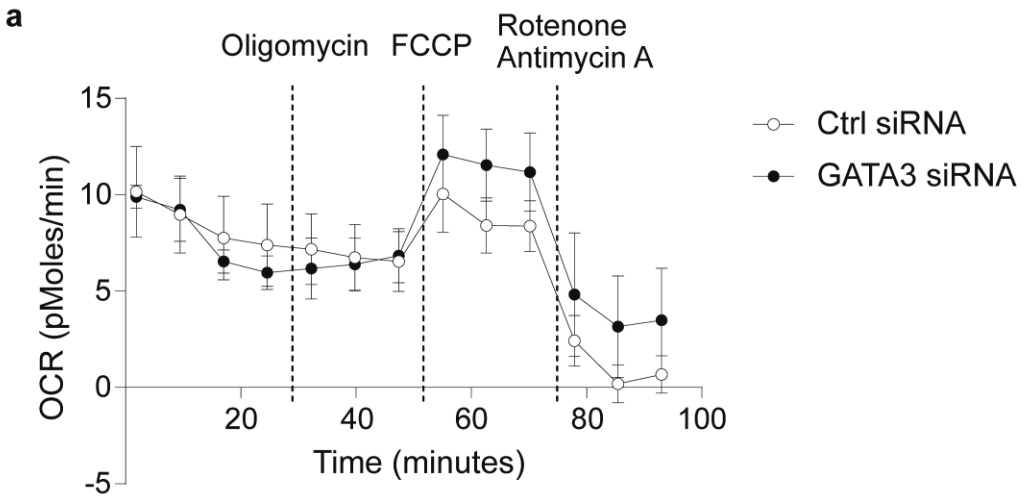
Supplementary figure 4.